Journal of Materials Chemistry C

Accepted Manuscript

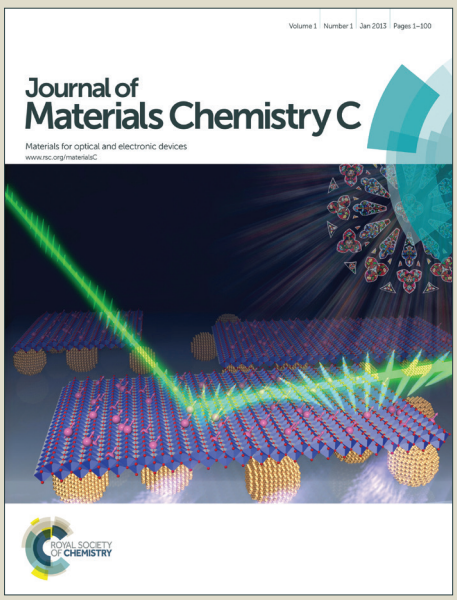

ROYAL SOCIETY OF CHEMISTRY

www.rsc.org/materialsC

Journal Name

RSCPublishing

ARTICLE

Molecular doping of ZnO by ammonia: A possible shallow acceptor

Cite this: DOI: 10.1039/x0xx00000x

Junhyeok Bang,[a] Yi-Yang Sun,[*a] Damien West,[a] Bruno K. Meyer,[b] and Shengbai Zhang[*c]

Received 00th January 2012,
Accepted 00th January 2012

DOI: 10.1039/x0xx00000x

www.rsc.org/

Stable p-type doping of ZnO has been a major technical barrier for the application of ZnO in optoelectronic devices. While p-type conductivity for nitrogen-doped ZnO has been repeatedly reported, its origin remains to be mysterious. Here, using first-principles calculation, we predict that an ammonia molecule could counterintuitively assume a Zn site and form a substitutional defect, $(NH_3)_{Zn}$. By comparing with other molecular dopants (N_2 and NO) on Zn site and N on O site (N_O), we found that $(NH_3)_{Zn}$ is thermodynamically the most stable defect under O-rich condition. The stability is attributed to the formation of a strong dative bond of the ammonia molecule with a neighbouring O atom. The $(NH_3)_{Zn}$ defect is neutral regardless of the Fermi level of the system, but it can capture a H donor forming $(NH_4)_{Zn}$, which becomes an acceptor. Experimental evidence for the existence of this Zn-site N acceptor is provided based on a comparison of calculated and measured N 1*s* X-ray photoelectron spectra. Accurately calculating the (0/-) transition level for this and other N-based acceptors has been hindered by the theoretical method used. Experimental studies are called for to clarify on its (0/-) transition level.

Introduction

Zinc oxide (ZnO) exhibits the well-known doping asymmetry problem,[1] which has also been observed in other wide band gap semiconductors (usually to a lesser extent).[2] While *n*-type doping in ZnO can be readily achieved, *p*-type doping is notoriously difficult and unstable,[3] which hinders the long-envisaged application of ZnO in optoelectronic devices.[4] Doping by group-V elements is considered to be the most promising approach to achieving *p*-type ZnO[5] and has been intensively studied in recent years. Hole concentrations of 10^{16} – 10^{18} cm^{-3} have been reported, for example, by using nitrogen doping.[6-9] Such *p*-type conductivity was originally thought to be caused by N substitution for O (N_O). Previous density functional calculations suggested that N_O has a relatively shallow acceptor level as low as 0.3 eV above the valence band maximum (VBM).[1,10,11] However, recent hybrid functional calculations, which typically yield improved band gaps for semiconductors, showed that N_O is a deep acceptor with a transition level of 1.3 eV above the VBM.[12] This deep-acceptor model for N_O is supported by a recent photoluminescence experiment.[13] So far, the origin of the *p*-type conductivity in N-doped ZnO remains to be mysterious.

Previous studies on N-doping in ZnO have focused on N or N-containing small molecules (such as NO or N_2) substituting at an O site. Considering the deep level associated with N_O, one should be cautious now to take the view that N and O are always chemically similar in terms of doping. As a matter of fact, N_O seldom behaves as a shallow acceptor in natively *n*-type oxides.[14,15] Instead, N doping is commonly used to reduce the band gap by introducing deep levels.[16,17] It is thus meaningful to study other possible forms of existence of N in ZnO. Having N acceptors occupy Zn sites is counter-intuitive and has been rarely studied. However, even though it is energetically not favoured to have a bare N atom occupying a Zn site, N-containing molecules could be suited at Zn sites. A possible type of defects that has been overlooked in previous studies is ammonia (NH_3) as a molecular dopant. The flexibility of the lone-pair electrons of NH_3 in forming chemical bonds makes it amenable to both Zn and O sites in ZnO. Since NH_3 is often used as the N-dopant for *p*-type ZnO,[6,18-21] it is of great interest to study the properties of such defects.

In this work, using first-principles calculation we study the molecular doping of NH_3 in ZnO. Other molecule dopants, e.g., N_2 and NO, have been previously studied at the O site[10,24] as they are also commonly used sources for N in attempting to obtain *p*-type ZnO.[22,23] Studies at the Zn site has been rare except a very recent study of N_2 substitution for Zn.[25] Here, we study the atomic and electronic structures of these Zn-site N acceptors in ZnO. We compare the thermodynamic stabilities of these defects with other proposed N acceptors. It is found that the NH_3 molecule at Zn site could strongly bind with a neighbouring O atom through the lone-pair electrons of N, which makes the $(NH_3)_{Zn}$ defect is significantly stabilized over a bare Zn vacancy (V_{Zn}). Our study on the thermodynamic stability shows that $(NH_3)_{Zn}$ is the most stable N defect under O-rich growth condition, which is the typical condition for growing *p*-type ZnO in order to avoid the formation of O vacancies. Furthermore, our study has revealed a rich chemistry of NH_3 in ZnO. $(NH_3)_{Zn}$ can capture an additional H atom to

form the acceptor $(NH_4)_{Zn}$ or NH_3 can occupy the O site and become a shallow donor. According to our calculation, $(N_2)_{Zn}$, $(NO)_{Zn}$ and $(NH_4)_{Zn}$ are all acceptors. The calculated ionization energy of these defects, however, strongly relies on the theoretical method used. The acceptor levels from hybrid functional calculations are significantly deeper than those from semi-local functional (including Hubbard U) calculations. Experimental studies are called for to examine these results. Lastly, we show the experimental evidence for the existence of the $(NH_4)_{Zn}$ defect by re-analysing the experimental N 1*s* X-ray photoelectron spectra (XPS) from the literature.

Computational method

Our first-principles calculation was based on the density functional theory (DFT) as implemented in the VASP program.[26] The generalized gradient approximation of Perdew, Burke and Ernzerhof (PBE) was used for the exchange-correlation functional.[27] The band gap of ZnO from the PBE calculation is 0.72 eV, which is significantly smaller than the experimental value (3.43 eV). To partially correct this error, we applied the PBE+U method[28] with U=8.0 eV and J=0.9 eV, as derived from first-principles calculations for Zn 3*d* electrons.[29] The PBE+U method lowers the Zn 3*d* band and hence the VBM of ZnO as a result of reduced *p*-*d* coupling. The band gap from the PBE+U calculation is 1.73 eV. For selected cases, we performed calculations using the hybrid functional of Heyd, Scuseria and Ernzerhof (HSE),[30] where a mixing parameter of 0.375 for the Hartree-Fock exchange[31] is used to reproduce the experimental band gap of 3.43 eV. The results reported below are from PBE+U calculations unless stated otherwise.

Projector augmented wave (PAW) potentials[32] were used to describe the core-valence interaction and plane-waves up to kinetic energy of 408 eV were used as the basis set. A (5×5×3) 300-atom supercell was used to model the defects. The calculated lattice constants (a=3.289 Å and c=5.311 Å from PBE, a=3.209 Å and c=5.162 Å from PBE+U, and a=3.249 Å and c=5.218 Å from HSE) were used to set up the supercells. The Brillouin zone was represented by the Γ point. The atomic structures were relaxed until the residual forces on all atoms were smaller than 0.025 eV/Å (0.05 eV/ Å in HSE calculations).

Results and discussion

Atomic and electronic structures. We start with comparing the atomic and electronic structures of different N acceptors on Zn-site, which is helpful to the discussion of the chemical bonding and thermodynamic stability of these defects. Figure 1 shows the atomic structures for V_{Zn}, which can be considered as the parent defect, and the three N acceptors on Zn site studied in this work. Figure 2 shows the corresponding electronic structures for the four defects. V_{Zn} has been widely studied in previous works. Here we give a brief summary of our results on this defect. In the neutral charge state, V_{Zn} maintains the C_{3v} point symmetry and the double degeneracy at the VBM.[33] The topmost doubly-degenerate spin-down orbitals are empty making V_{Zn} a double acceptor. Figure 1(a) also shows the wavefunctions of the two degenerate empty (hole) states, which are mainly localized on the three non-axial O atoms next to V_{Zn}. There is another occupied state localized on the axial O next to V_{Zn}, which is just slightly lower than the two empty states. This state is the split-off state due to the T_d-to-C_{3v} transition of the local symmetry in the wurtzite structure.

When the Zn vacancy is occupied by a N_2 or NO molecule, the local C_{3v} symmetry is reduced to C_s symmetry with only a mirror plane. Two of the neighbouring O atoms are on the mirror plane, while the other two are out of the plane and mirrored to each other. As a result of the lowered symmetry, the double degeneracy of the VBM is lifted. As can be seen in Fig. 2, the topmost two spin-down orbitals are split up for $(N_2)_{Zn}$ and $(NO)_{Zn}$. In the case of $(N_2)_{Zn}$, it remains to be a double acceptor because N_2 is a saturated molecule and does not donate electrons to or take electrons from the system. In the case of $(NO)_{Zn}$, because NO is a radical molecule having a dangling 2*p* electron, the defect can be either a triple or a single acceptor. Our calculation shows that $(NO)_{Zn}$ is a single acceptor meaning that NO donates its dangling electron to V_{Zn}.

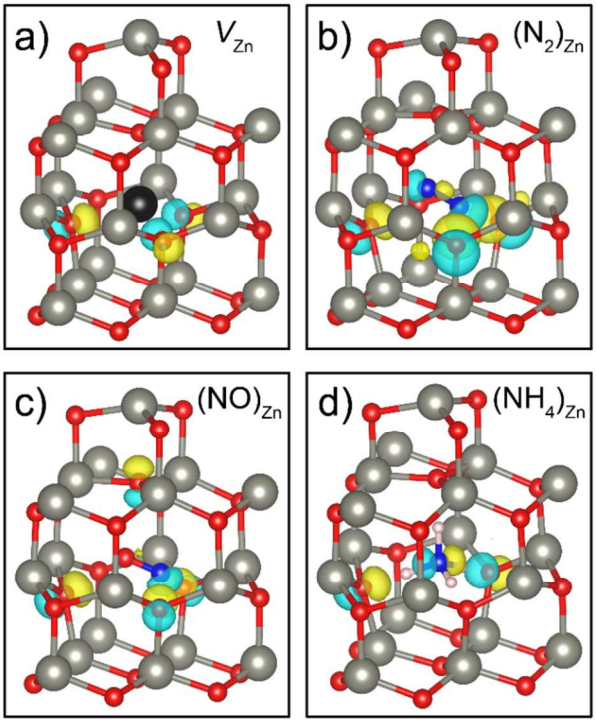

Fig. 1 Atomic structures of V_{Zn} (a) and the Zn-site N acceptors in ZnO. (b) $(N_2)_{Zn}$, (c) $(NO)_{Zn}$, and (d) $(NH_4)_{Zn}$. Zn, O, N, and H atoms are represented by gray (large), red (medium), blue (medium) and pink (small) balls, respectively. The Zn vacancy in (a) is marked by a black ball. The wavefunctions of the acceptor hole states are plotted together with the atomic structure, where the yellow and cyan colours represent the positive and negative parts of the wavefunctions, respectively.

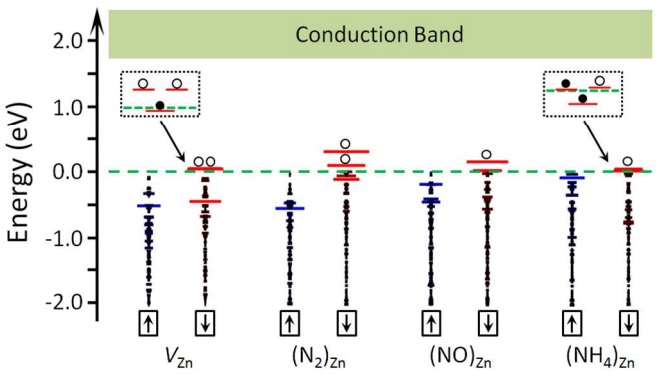

Fig. 2 Electronic structures (eigenvalue spectrum at the Γ point of the Brillouin zone of the 300-atom supercell) of V_{Zn} and the Zn-site N acceptors in ZnO. Each state is represented by a horizontal bar. The width of a bar represents the projection of the state on the four O atoms next to the Zn vacancy. A large projection is also highlighted by blue color for spin-up states and red color for spin-down states. The two insets in dashed-line boxes show zoom-in views of the spin-down states near the VBM.

The presence of N_2 or NO pushes all the four neighbouring O atoms outward. The displacement of the axial O atom (about 38%) is more prominent than that of the non-axial O atoms (about 12-24 %). As can be seen from the wavefunctions shown in Fig. 1, both N_2 and NO couple with the V_{Zn} states. But, the change in bond length compared with the isolated molecules is small. The N-N and N-O bond lengths in $(N_2)_{Zn}$ and $(NO)_{Zn}$ defects are 1.13 Å and 1.16 Å, respectively, while the corresponding values in isolated molecules are 1.12 Å and 1.17 Å, respectively. This small change in bond length is possibly a result of cancelation of electronic screening effect, which tends to dilate the bond length, and the steric hindrance, which tends to restrain the change in bond length.

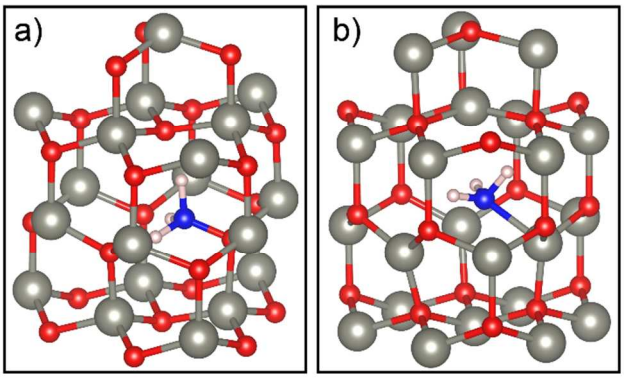

Fig. 3 Atomic structures of (a) $(NH_3)_{Zn}$ and (b) $(NH_3)_O$ in ZnO.

Now, consider a NH_3 molecule occupying a Zn site. An isolated NH_3 molecule has two lone-pair electrons in a nonbonding orbital, which are considerably higher in energy than the three bonding orbitals between N and H. Thus, NH_3 can be viewed as having two valence electrons and isovalent with Zn. When occupying a Zn site, NH_3 can donate the two lone-pair electrons and fill the two holes created by V_{Zn} (see Fig. 2). Our calculation indeed shows that $(NH_3)_{Zn}$ is a neutral defect in ZnO regardless of the Fermi level. Figure 3(a) shows the optimized atomic structure of the $(NH_3)_{Zn}$ defect, where the N atom forms a bond with a non-axial O atom and NH_3 maintains its molecular form. It is worth to note that NH_3 can also occupy an O site forming $(NH_3)_O$, as shown in Fig. 3(b), which is a shallow donor with the (0/+) transition level nearly at the CBM from both PBE and PBE+U calculations.

The $(NH_3)_{Zn}$ defect can react with other defects in ZnO, such as interstitial hydrogen (H_i), which is known to exist in ZnO in significant amount and are mobile.[33,34] When $(NH_3)_{Zn}$ captures a H atom, the N-O bond is broken and the additional H atom binds to the N atom to form the $(NH_4)_{Zn}$ defect. The atomic structure of this defect is shown in Fig. 1(d). All the four neighbouring O atoms relax outward. For an isolated NH_4 radical, the four N-H bonding orbitals are low in energy and the high-lying anti-bonding orbital is occupied by one electron, which is ready to be donated. In this sense, the NH_4 molecule is analogous to a group-I element and behaves as a single acceptor when occupying a Zn site.

Figure 2 shows the electronic structure of the $(NH_4)_{Zn}$ defect. Similar to V_{Zn}, there are three states near the VBM, where two are nearly degenerate and another one is slightly lower in energy. The topmost two states are split up because of the Jahn-Teller distortion with the upper one empty and the lower one occupied. However, the level splitting is negligibly small. The distortion results in a reduction of symmetry from C_{3v} to C_s. But, different from the cases of $(N_2)_{Zn}$ and $(NO)_{Zn}$, the distortion in $(NH_4)_{Zn}$ is driven by the electronic effect (i.e, Jahn-Teller effect). As a result of the distortion, the bond length between N and one of the non-axial H atoms is slightly longer (by about 0.002 Å) than those between N and the other two non-axial H atoms. Figure 1(d) shows the wavefunction of the empty state. It can be seen that this state is localized only on the two non-axial O atoms out of the mirror plane.

Thermodynamic stability. We calculate the formation energy of a defect (D) in a charge state q according to[35]

$$E^{\text{form}}(\text{D}^q) = E(\text{D}^q) - E_{\text{bulk}} + \sum_i \Delta n_i \mu_i + q(E_{\text{F}} + E_{\text{VBM}})$$

where $E(\text{D}^q)$ and E_{bulk} are the total energies of the defect-containing and defect-free supercells, respectively, Δn_i is the quantity of the i-th species exchanged in forming the defect and μ_i is the chemical potential of the i-th species. The Fermi level, E_F, is referenced to the VBM energy, E_{VBM}, of the defect-free supercell. We consider μ_{N_2}, μ_{NO} and μ_{NH_3} to be the total energies of corresponding isolated molecules, while μ_{Zn} and μ_O, as referenced to bulk Zn and an isolated O_2 molecule, respectively, are allowed to vary between 0 and ΔH(ZnO), which is the enthalpy of formation of bulk ZnO, with the constraint that $\mu_{Zn} + \mu_O = \Delta H$(ZnO). The calculated ΔH(ZnO) from PBE+U calculation is 3.60 eV/ZnO, in good agreement with experiment.[36]

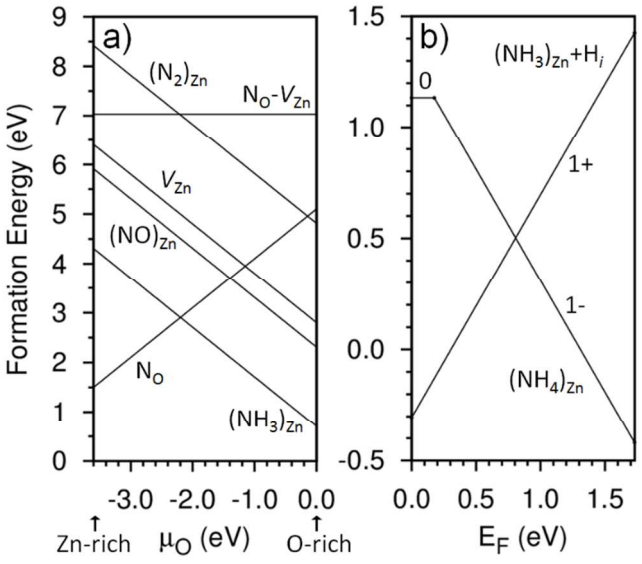

Fig. 4 (a) Formation energy of Zn-site and O-site N-related defects as a function of O chemical potential (μ_O). All defects are calculated at the neutral charge state. (b) Comparison of the formation energy of $(NH_4)_{Zn}$ and the

sum of the formation energies of isolated $(NH_3)_{Zn}$ and H_i as a function of Fermi level (E_F).

Figure 4(a) shows the calculated formation energies of the Zn-site defects studied in this work and two O-site acceptors, N_O and N_O-V_{Zn} complex, the latter of which has been recently proposed to account for the *p*-type conductivity in N-doped ZnO.[37,38] From these results, $(NH_3)_{Zn}$ has the lowest formation energy in the Zn-site defects. The lowering of the formation energy from V_{Zn} by 2.09 eV is due to the binding of NH_3 to an O atom. It is also energetically favourable with NO sitting at a V_{Zn}, for which the energy lowering is about 0.56 eV. The interaction of N_2 with V_{Zn} is purely repulsive making the formation energy of $(N_2)_{Zn}$ much higher than V_{Zn}. Under the Zn-rich condition, N_O becomes the most stable defect. The N_O-V_{Zn} complex is independent of the chemical potentials and has rather high formation energy. Therefore, the creation of this complex relies on the kinetic mechanism as discussed in Ref. 37.

We now consider the binding of $(NH_3)_{Zn}$ with a hydrogen interstitial (H_i) to form $(NH_4)_{Zn}$. Hydrogen exists in ZnO in significant amount and plays an important role in the native *n*-type conductivity. To make *p*-type ZnO, it is necessary to deactivate the hydrogen donors. Forming $(NH_4)_{Zn}$ is a possible route achieving this. The formation energy of $(NH_4)_{Zn}$ from $(NH_3)_{Zn}$ and H_i is independent of the chemical potentials, but depends on the Fermi level of the system. Figure 4(b) shows the formation energy of $(NH_4)_{Zn}$ as a function of E_F at O-rich condition. It can be seen that the formation of $(NH_4)_{Zn}$ is more favourable when E_F is closer to the CBM (*n*-type condition), while $(NH_4)_{Zn}$ tends to dissociate into $(NH_3)_{Zn}$ and H_i when E_F is closer to the VBM (*p*-type condition). This result suggests that incorporation of NH_3 in ZnO can at least compensate the hydrogen donors. Whether it can convert ZnO to *p*-type depends on the transition level (or ionization energy) of the $(NH_4)_{Zn}$ defect.

TABLE I. The calculated (0/-) transition levels of V_{Zn} and N acceptors in ZnO from PBE and PBE+*U* calculations. The unit is eV. The reference energy is the VBM.

ε(0/-)	V_{Zn}	$(N_2)_{Zn}$	$(NO)_{Zn}$	$(NH_4)_{Zn}$	N_O	N_O-V_{Zn}
PBE	0.06	0.04	0.03	0.04	0.32	0.16
PBE+*U*	0.17	0.22	0.23	0.18	0.57	0.33

Acceptor ionization energy. We calculated the transition level from neutral to 1- charge state, ε(0/-), for the defects discussed above according to $\varepsilon(0/-) = E(D^-) - E(D^0) - E_{VBM}$.[35] Table I lists the results obtained from PBE and PBE+*U* calculations. The error due to the image-charge interaction is estimated to be in the range of 0-70 meV using a Madelung correction,[39] which is not included in Table I. From the PBE results, all Zn-site acceptors have shallow (0/-) transition levels, while both N_O and N_O-V_{Zn} show relatively deep transition levels. In PBE+*U* calculation, the transition levels become noticeably deeper than those from PBE. Even though the PBE+*U* results already indicate characters of non-hydrogenic defects, the calculated transition levels are still in the range where *p*-type conductivity can be expected.

In contrast to PBE and PBE+*U* results, the transition levels from HSE calculations are drastically deeper as a result of the significant charge localization effect due to the Hartree-Fock exchange mixed into the HSE functional.[40] In the case of $(NH_4)_{Zn}$, the ε(0/-) level from HSE calculation is 1.22 eV above the VBM. Meanwhile, the negligible Jahn-Teller distortion as found in PBE+*U* calculation becomes much more prominent in HSE calculation. As a result, the two H atoms on the mirror plane depart from the N atom and form bonds with the neighbouring O atoms. Because of this large structural relaxation, the hole state is lifted up from near the VBM (in PBE+*U* calculation, see Fig. 2) to near the CBM (in HSE calculation).

It is unclear if the large distortion in the HSE calculation represents the actual situation or an artifact due to over-localization of electronic states. In a recent work by Lambrecht and Boonchun,[25] the authors also found that for $(N_2)_{Zn}$ the PBE transition level is relatively shallow, while the HSE transition level is deep. We have obtained even deeper transition level (1.42 eV) for $(N_2)_{Zn}$ in HSE calculation, which is a combined result of a larger mixing parameter used in our HSE functional than that in Ref. 25 and a spin polarization in the neutral charge state. Based on the analysis of the fulfilment of the generalized Koopmans theorem and comparison with electron paramagnetic resonance experiment,[41] Lambrecht and Boonchun have concluded that PBE results should be preferred in the case of Zn-site acceptors.

Another possible shallow N-acceptor is the N_O-V_{Zn} complex proposed by Liu *et al.*[37] Different from the cases of $(NH_4)_{Zn}$ and $(N_2)_{Zn}$ discussed above, both PBE and HSE calculations suggested that N_O-V_{Zn} be a shallow acceptor with the ε(0/-) level at 0.11 and 0.16 eV above the VBM, respectively.[37] It is noted that the shallow transition energy can only be obtained by forcing the defect to be non-magnetic in the calculation, which was assumed in Ref. 37 by arguing that there is no long-range ferromagnetism between the defects. Given the unpaired electrons, however, this defect complex individually should still be a paramagnetic centre. If we remove the assumption of being non-magnetic by performing a spin-polarized calculation, the ε(0/-) level becomes 0.87 eV above the VBM using the 72-atom supercell as in Ref. 37. We also increased the supercell size for N_O-V_{Zn} to 300 atoms in our HSE calculation and obtained a transition level of 1.26 eV above the VBM.

With the results above and the previous HSE result on the N_O defect,[12] we reach the conclusion that HSE functional would yield deep levels (at least 1.2 eV above the VBM) for all the proposed N-acceptors. This is, however, in contrast to the repeated report of shallow acceptors in N-doped ZnO with the transition level in the range from 0.13 to 0.20 eV.[7,19,38,42,43] In particular, Reynolds *et al.* showed Raman signal of the N_O-V_{Zn}-H complex and, based on photoluminescence measurement, assigned an acceptor level of 134 meV to this defect complex.[38] Given this unresolved issue, we are reserved to interpret the HSE results for this particular system.

Correlation to experimental results. Experimentally, the occupation site and the chemical states of the N dopants have been commonly characterized by the N 1*s* binding energy from XPS. Perkins *et al.* performed a dedicated comparative XPS study on ZnO samples prepared by reactive sputtering and metalorganic chemical vapour deposition (MOCVD).[44] In the sputtering-produced samples, two N 1*s* peaks, one at 404.9 eV and another at 396.5 eV, were observed. The 404.9-eV peak was assigned to the $(N_2)_O$ defect, while the 396.5-eV peak was assigned to the N_O defect. The assignments were based on a comparison with the XPS spectrum from N_2^+ implanted Zn foil. In addition, the 396.5-eV peak is also close to the N 1*s* peak in Zn_3N_2 thin film (395.8 eV).[45] In the MOCVD-grown samples, two extra N 1*s* peaks, one at 398.3 and another at 399.5 eV, were observed. These two peaks have also been reported in a number of other XPS studies with the assignments still

elusive.[43,46–50] The involvement of N-C and N-H bonds in the 398.3-eV and 399.5-eV peaks, respectively, have been discussed because C and H are the most common unintentional dopants in the growth techniques such as MOCVD. Two issues, however, arise from the N-C and N-H assignments: 1) Can replacing one N by C in $(N_2)_O$ forming $(CN)_O$ lower the 404.9-eV peak by 6.6 eV to 398.3 eV? 2) Can adding one H to the N in N_O push the 396.5-eV peak by 3.0 eV to 399.5 eV? XPS studies on the adsorption of different NH_x species (x=1-4) on ZnO and other surfaces show that the N 1*s* binding energy typically increases by about 1 eV in the range from 398.0 to 402.5 eV when x is increased by one.[51–54]

We calculated N 1*s* core-level shifts for different N defects within the final-state approximation[55] using Slater's transition-state concept.[56] Even though the calculated absolute binding energy may not be accurate, the difference between the binding energies can be more reasonable. For the N_O and $(N_2)_O$ defects, we obtained a difference of about 7 eV for their corresponding N 1*s* peaks to be compared with the experimental value of about 8 eV.[44] For $(N_2)_O$ and $(CN)_O$ defects, it has been shown that they adopted the split-interstitial configuration.[24] With this structure, we found a downshift of N 1*s* peak in $(CN)_O$ by only 2.4 eV from that in $(N_2)_O$, suggesting that $(CN)_O$ may not account for the peaks below 400 eV. Moreover, we found that the N_O-H complexes with H at the bond-centre and anti-bonding sites[34] produce a N 1*s* peak at 397.8 and 398.3 eV, respectively, in better agreement with the experimental peak at 398.3 eV. This result suggests that a single N-H bond may not be sufficient to generate an upshift of N 1*s* level by 3 eV to account for the peak at 399.5 eV. In contrast, the N 1*s* peak calculated for the $(NH_4)_{Zn}$ defect is 2.7 eV deeper than that of N_O, i.e., at 399.2 eV, which is in better agreement with the experimental 399.5-eV peak.

Conclusions

In summary, using first-principles calculation we studied molecular doping of ZnO by NH_3, which has been compared with other possible N defects in ZnO. Our study revealed rich chemistry of NH_3 in ZnO. NH_3 can be viewed as isovalent to Zn. Our calculation showed that NH_3, when occupying a Zn site, can donate its lone-pair electrons to fill the two holes created by V_{Zn} and form a strong dative bond to a neighbouring O. This makes $(NH_3)_{Zn}$ thermodynamically the most stable N-related defect in ZnO under O-rich condition. Second, $(NH_3)_{Zn}$ can capture a H donor under *n*-type condition to form $(NH_4)_{Zn}$, which becomes an acceptor. The $(NH_4)_{Zn}$ defect was suggested to account for the N 1*s* peak around 399.5 eV in XPS experiments. The calculated (0/-) transition level is strongly dependent on the theoretical method used. It is worth of experimental efforts to resolve this issue.

Acknowledgements

JB, DW and SBZ were supported by US Department of Energy (DOE) under Grant No. DE-SC0002623. YYS acknowledges support from National Science Foundation under Award No. DMR-1104994. The supercomputer time was provided by the National Energy Research Scientific Computing Center (NERSC) under DOE Contract No. DE-AC02-05CH11231 and the Center for Computational Innovations (CCI) at Rensselaer Polytechnic Institute.

Notes and references

[a] Department of Physics, Applied Physics, & Astronomy, Rensselaer Polytechnic Institute, Troy, New York 12180, USA.
[b] Physics Institute, Justus Liebig University Gießen, Heinrich-Buff-Ring 16, 35392 Gießen, Germany.
* Emails: suny4@rpi.edu (YYS); zhangs9@rpi.edu (SBZ)

1 S. B. Zhang, S.-H. Wei, and A. Zunger, *Phys. Rev. B*, 2001, **63**, 075205.
2 S. B. Zhang, S.-H. Wei, and A. Zunger, *J. Appl. Phys.*, 1998, **83**, 3192.
3 D. C. Look, B. Claflin, Y. I. Alivov, and S. J. Park, *Phys. Stat. Sol. (a)*, 2004, **201**, 2203.
4 D.C. Look, *Mater. Sci. Eng. B*, 2001, **80**, 383.
5 D. C. Look and B. Claflin, *Phys. Stat. Sol. (b)*, 2004, **241**, 624.
6 K. Minegishi, Y. Koiwai, Y. Kikuchi, K. Yano, M. Kasuga, and A. Shimizu, *Jpn. J. Appl. Phys.*, 1997, **36**, L1453.
7 D. C. Look, D. C. Reynolds, C. W. Litton, R. L. Jones, D. B. Eason, and G. Cantwell, *Appl. Phys. Lett.*, 2002, **81**, 1830.
8 T. M. Barnes, K. Olson, and C. A. Wolden, *Appl. Phys. Lett.*, 2005, **86**, 112112.
9 B. Yao, et al., *J. Luminescence*, 2007, **122-123**, 191.
10 E. C. Lee, Y. S. Kim, Y. G. Jin, and K. J. Chang, *Phys. Rev. B*, 2001, **64**, 085120.
11 J. Li, S. H. Wei, S. S. Li, and J. B. Xia, *Phys. Rev. B*, 2006, **74**, 081201.
12 J. L. Lyons, A. Janotti, and C. G. Van de Walle, *Appl. Phys. Lett.*, 2009, **95**, 252105.
13 M. C. Tarun, M. Z. Iqbal, and M. D. McCluskey, *AIP Adv.*, 2011, **1**, 022105.
14 D. O. Scanlon and G. W. Watson, *J. Mater. Chem.*, 2012, **22**, 25236.
15 C. Di Valentin, G. Pacchioni, A. Selloni, S. Livraghi, and E. Giamello, *J. Phys. Chem. B*, 2005, **109**, 11414.
16 R. Asahi, T. Morikawa, T. Ohwaki, K. Aoki, and Y. Taga, *Science*, 2001, **293**, 269.
17 K. R. Reyes-Gil, E. A. Reyes-Garcia, and D. Raftery, *J. Phys. Chem. C*, 2007, **111**, 14579.
18 A. Zeuner, H. Alves, D. M. Hofmann, B. K. Meyer, A. Hoffmann, U. Haboeck, M. Strassburg, and M. Dworzak, *Phys. Stat. Sol. (b)*, 2002, **234**, R7.
19 S. Lautenschlaeger, S. Eisermann, B. K. Meyer, G. Callsen, M. R. Wagner, and A. Hoffmann, *Phys. Stat. Sol. (RRL)*, 2009, **3**, 16.
20 S. Lautenschlaeger, M. Hofmann, S. Eisermann, G. Haas, M. Pinnisch, A. Laufer, and B. K. Meyer, *Phys. Stat. Sol. (b)*, 2011, **248**, 1217.
21 K. Nakahara, et al., *Appl. Phys. Lett.*, 2010, **97**, 013501.
22 A. Tsukazaki, et al., *Nature Mater.*, 2005, **4**, 42.
23 X. Li, Y. Yan, T. A. Gessert, C. DeHart, C. L. Perkins, D. Young, and T. J. Coutts, Electrochem. *Solid-State Lett.*, 2003, **6**, C56.
24 S. Limpijumnong, X. Li, S.-H. Wei, and S. B. Zhang, *Appl. Phys. Lett.*, 2005, **86**, 211910.
25 W. R. L. Lambrecht and A. Boonchun, *Phys. Rev. B*, 2013, **87**, 195207.
26 G. Kresse and J. Furthmüller, *Comp. Mater. Sci.*, 1996, **6**, 15.
27 J. P. Perdew, K. Burke, and M. Ernzerhof, *Phys. Rev. Lett.*, 1996, **77**, 3865.
28 S. L. Dudarev, G. A. Botton, S. Y. Savrasov, C. J. Humphreys, and A. P. Sutton, *Phys. Rev. B*, 1998, **57**, 1505.

29 B.-C. Shih, Y. Xue, P. Zhang, M. L. Cohen, and S. G. Louie, *Phys. Rev. Lett.*, 2010, **105**, 146401.
30 J. Heyd, G. E. Scuseria, and M. Ernzerhof, *J. Chem. Phys.*, 2003, **118**, 8207.
31 F. Oba, A. Togo, I. Tanaka, J. Paier, and G. Kresse, *Phys. Rev. B*, 2008, **77**, 245202.
32 G. Kresse and D. Joubert, *Phys. Rev. B*, 1999, **59**, 1758 (1999).
33 J. Bang and K. J. Chang, *Appl. Phys. Lett.*, 2008, **92**, 132109.
34 C. G. Van de Walle, *Phys. Rev. Lett.*, 2000, **85**, 1012.
35 S. B. Zhang and J. E. Northrup, *Phys. Rev. Lett.*, 1991, **67**, 2339.
36 J. D. Cox, D. D. Wagman, and V. A. Medvedev, *CODATA Key Values for Thermodynamics*, (Hemisphere Publishing Corp., New York, 1989).
37 L. Liu, et al., *Phys. Rev. Lett.*, 2012, **108**, 215501.
38 J. G. Reynolds, C. L. Reynolds, Jr., A. Mohanta, J. F. Muth, J. E. Rowe, H. O. Everitt, and D. E. Aspnes, *Appl. Phys. Lett.*, 2013, **102**, 152114.
39 M. Leslie and M. J. Gillan, *J. Phys. C*, 1985, **18**, 973.
40 P. Mori-Sánchez, A. J. Cohen, and W. Yang, *Phys. Rev. Lett.*, 2008, **100**, 146401.
41 N. Y. Garces, L. Wang, N. C. Giles, L. E. Halliburton, G. Cantwell and D. B. Eason, *J. Appl. Phys.*, 2003, **94**, 519.
42 A. Kurtz, A. Hierro, E. Munoz, S. K. Mohanta, A. Nakamura, and J. Temmyo, *Appl. Phys. Lett.*, 2014, **104**, 081105.
43 P. Cao, D. X. Zhao, J. Y. Zhang, D. Z. Shen, Y. M. Lu, B. Yao, B. H. Li, Y. Bai, X. W. Fan, *Appl. Surf. Sci.*, 2008, **254**, 2900.
44 C. L. Perkins, S.-H. Lee, X. Li, S. E. Asher, and T. J. Coutts, *J. Appl. Phys.*, 2005, **97**, 034907.
45 M. Futsuhara, K. Yoshioka, and O. Takai, *Thin Solid Films*, 1998, **322**, 274–281.
46 G. W. Cong, W. Q. Peng, H. Y. Wei, X. X. Han, J. J. Wu, X. L. Liu, Q. S. Zhu, Z. G. Wang, J. G. Lu, Z. Z. Ye, L. P. Zhu, H. J. Qian, R. Su, C. H. Hong, J. Zhong, K. Ibrahim, and T. D. Hu, *Appl. Phys. Lett.*, 2006, **88**, 062110.
47 J. P. Zhang, L. D. Zhang, L. Q. Zhu, Y. Zhang, M. Liu, X. J. Wang, and G. He, *J. Appl. Phys.*, 2007, **102**, 114903.
48 Z. P. Wei, B. Yao, Z. Z. Zhang, Y. M. Lu, D. Z. Shen, B. H. Li, X. H. Wang, J. Y. Zhang, D. X. Zhao, X. W. Fan, and Z. K. Tang, *Appl. Phys. Lett.*, 2006, **89**, 102104.
49 J. Wang, E. Elamurugu, V. Sallet, F. Jomard, A. Lusson, A. M. B. do Rego, P. Barquinha, G. Gonçalves, R. Martins, and E. Fortunato, *Appl. Surf. Sci.*, 2008, **254**, 7178.
50 W. Li, C. Kong, G. Qin, H. Ruan, and L. Fang, *J. Alloys Compd.*, 2014, **609**, 173.
51 U. Diebold and T. E. Madey, *J. Vac. Sci. Technol. A*, 1992, **10**, 2327.
52 A. Galtayries, E. Laksono, J.-M. Siffre, C. Argile, and P. Marcus, *Surf. Interface Anal.*, 2000, **30**, 140.
53 C. Guimon, A. Gervasini, and A. Auroux, *J. Phys. Chem. B*, 2001, **105**, 10316.
54 K. Ozawa, T. Hasegawa, K. Edamoto, K. Takahashi, and M. Kamada, *J. Phys. Chem. B*, 2002, **106**, 9380.
55 L. Köhler and G. Kresse, *Phys. Rev. B*, 2004, **70**, 165405.
56 It has been shown that (S. B. Zhang, S.-H. Wei, and A. Zunger, *Phys. Rev. B*, 1995, **52**, 13975.) for ZnO the use of Slater transition-state approximation yields better results for semi-core electrons when compared with experiment.